Resonance in a model for Cooker's sloshing experiment

by H. Alemi Ardakani, T.J. Bridges & M.R. Turner

Department of Mathematics, University of Surrey, Guildford, Surrey GU2 7XH, England

– Abstract –

Cooker's sloshing experiment is a prototype for studying the dynamic coupling between fluid sloshing and vessel motion. It involves a container, partially filled with fluid, suspended by two cables and constrained to remain horizontal while undergoing a pendulum-like motion. In this paper the fully-nonlinear equations are taken as a starting point, including a new derivation of the coupled equation for vessel motion, which is a forced nonlinear pendulum equation. The equations are then linearized and the natural frequencies studied. The coupling leads to a highly nonlinear transcendental characteristic equation for the frequencies. Two derivations of the characteristic equation are given, one based on a cosine expansion and the other based on a class of vertical eigenfunctions. These two characteristic equations are compared with previous results in the literature. Although the two derivations lead to dramatically different forms for the characteristic equation, we prove that they are equivalent. The most important observation is the discovery of an internal $1:1$ resonance in the fully two-dimensional finite depth model, where symmetric fluid modes are coupled to the vessel motion. Numerical evaluation of the resonant and nonresonant modes are presented. The implications of the resonance for the fluid dynamics, and for the nonlinear coupled dynamics near the resonance are also briefly discussed.

— April 25, 2012—

1 Introduction

In Cooker's sloshing experiment [11], a rectangular vessel containing fluid is suspended from a stationary beam by two cables which are free to rotate in a vertical plane. A schematic of the experiment is shown in Figure 1. The rectangular vessel has length L, height d, and unit width, and is partially filled with fluid of mean depth h_0. The tank is suspended by two rigid cables of equal length ℓ, and the cables make an angle θ with the vertical. The base of the tank remains horizontal during the motion.

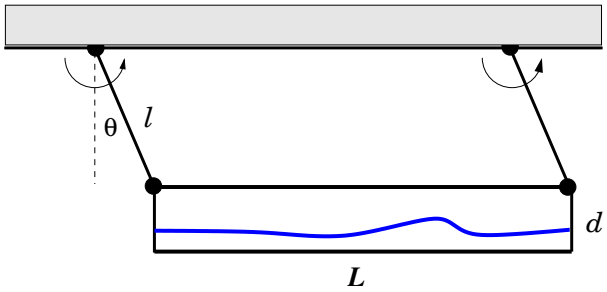

Figure 1: Schematic of Cooker's experimental configuration [11].

It is an experiment in the spirit of Taylor [26]: it is simple, easy to construct, robust and illuminates a fundamental question in fluid mechanics. In this case the question is the effect of vehicle coupling on fluid sloshing. Indeed, it is one of the simplest configurations that allows precise study of the coupled dynamics between the fluid motion and the vessel motion. The problem of sloshing in stationary vessels is already a very difficult problem to study both experimentally and theoretically (cf. Ibrahim [19] and Faltinsen & Timokha [12] and references therein). The coupled dynamics between fluid sloshing and vessel motion brings in a new dimension and the potential for enhancing or diminishing the sloshing motion through vehicle dynamics. The coupled problem is of great practical interest in the transport of liquids along roads, maritime fluid transport, and industrial applications. Hence a prototype for understanding the fundamentals of coupling is of great interest.

Cooker developed a linear theory of the coupled problem with a shallow-water model for the fluid. The theory showed that the coupling changed the set of natural frequencies, and the theory showed very good agreement with experimental results. Cooker's theory was extended by Alemi Ardakani & Bridges [3] to include a nonlinear shallow water model for the fluid, but the vessel model was still linear. A numerical algorithm for the simulation of the coupled problem was developed with careful attention taken to maintain the overall energy conservation and energy partition between fluid and vessel.

A related problem is that of *tuned liquid dampers* (TLDs). Ibrahim [19] gives a history of the many applications of TLDs with extensive references in §10.3.1 of [19]. The particular models of TLDs considered by Ikeda & Nakagawa [20] and Frandsen [13] are of interest here as their linearized models are equivalent to the linearized Cooker model. A schematic of a TLD is shown in Figure 2. A TLD consists of a vessel containing fluid, but constrained to move in the horizontal direction only, with the vessel motion governed by a linear spring-mass-damper model, and may include a horizontal forcing function. The nonlinear characteristics of TLDs are very different from Cooker's experiment, but at the

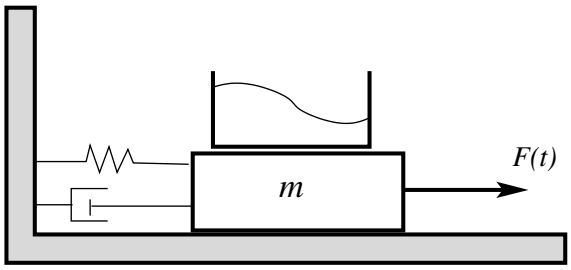

Figure 2: Schematic of a TLD system following Figure 1 of [13].

linear level the two systems are equivalent. Neglecting damping and forcing, and taking the fluid to be irrotational, the governing equations are exactly equivalent to the linearized equations governing Cooker's experiment. This equivalence is shown in §2.2. However the nonlinear equations are very different since the vessel motion in Cooker's experiment is fully nonlinear, governed by a forced pendulum equation (see equation (1.1) below), and includes vertical as well as horizontal motion.

Experiments for the case where the spring constant is zero have recently been reported by Herczyński & Weidman [18]. Spring constant zero corresponds to Cooker's experiment in the limit as the suspension length goes to infinity. These experiments are quite difficult because there is no restoring force and so the vessel may drift in addition to harmonic motion. Using a special low-friction cart, and carefully-controlled initial conditions, the experiments showed excellent agreement with the theory. However, without the spring force a 1:1 resonance, which is of great interest here, can not occur.

Ikeda & Nakagawa [20] used a modal expansion to study the nonlinear problem for TLDs. They included one anti-symmetric fluid mode, one symmetric fluid mode and the vessel mode, resulting in a $6-$dimensional system of nonlinear ODES. Their linear analysis is reviewed in §3. An infinite modal expansion for the linear TLD problem was first given by Frandsen [13]. The *linearized* TLD model in [13] is exactly equivalent to the *linearized* model for Cooker's experiment (cf. §2.2). The linear model and results of Frandsen [13] can be interpreted as the first reported results on the natural frequencies of a linear finite-depth model for Cooker's experiment. A cosine expansion is used and an infinite-product representation for the characteristic equation is presented, and numerical simulations of the nonlinear problem are presented. A key assumption in [13] is that symmetric modes are neglected since they exert no horizontal force on the vessel. We extend Frandsen's analysis by giving a new explicit sum representation for the characteristic equation and show moreover that the symmetric modes can be important when they couple to the vessel motion at resonance.

Independently, Yu [28] extended Cooker's model to include a fully two-dimensional model for the fluid, but restricted to linear fluid motion and linear vessel motion. Implicitly, an expansion in terms of "vertical eigenfunctions" [21] was used but the characteristic equation gives the same results as [13]. A range of results on the effect of fluid depth and mass ratio on the first mode were presented, showing a dramatic effect of finite but non-shallow depth.

The cosine expansion has as its organizing centre the cosine-eigenfunctions in the horizontal direction ($x-$direction) and the vertical eigenfunction expansion has as its organizing centre a class of eigenfunctions in the vertical direction ($y-$direction). The

two representations of the solution are very different. However, we prove, by constructing an explicit transformation, that the two representations are exactly equal. With this transformation we are able to show that the results of Frandsen [13] and Yu [28] are equivalent.

In previous work (e.g. [11, 20, 13, 28, 3]) there was some mystery about a "resonance". Cooker noted a curious resonance, where the second mode of the coupled problem resonated with the natural frequency of the dry vessel, but the resonance did not satisfy the characteristic equation. Frandsen [13] acknowledges that a resonance exists, but only considers the asymptotic case of small mass ratio (where the vessel mass is much greater than the fluid mass). Yu [28] disputed the role of resonance noting that there is no mechanism for continued energy input (see §3.5 of [28]).

In this paper the theory of Cooker's experiment in particular, and the theory of resonance in dynamic coupling in general, are extended in three directions. First, for the case of Cooker's experiment, a fully nonlinear model for the vessel motion is derived. It turns out to be a forced pendulum equation, with the forcing determined by the fluid pressure $p(x, y, t)$ on the vessel walls

$$\ddot{\theta} + \frac{g}{\ell} \sin\theta = \frac{1}{m_v \ell} \int_0^L \int_0^{h(x,t)} (p_x \cos\theta + p_y \sin\theta) \, \mathrm{d}y \mathrm{d}x \,, \tag{1.1}$$

where $y = h(x, t)$ is the position of the fluid free surface in the vessel, and g is the gravitational constant. Secondly, the coupled fluid-vessel equations for Cooker's experiment are linearized and a new derivation of the coupled characteristic equation is given. The cosine expansion approach is compared with the vertical eigenfunction approach and shown to be equivalent. Thirdly, we have discovered that there is a resonance, where the uncoupled symmetric fluid mode resonates exactly with an anti-symmetric fluid mode joined with the vessel motion. It is an *internal resonance*, where two natural frequencies are equal and have linearly independent eigenvectors. In the dynamical systems literature it is called a $1:1$ resonance, or sometimes the $1:1$ semisimple resonance (e.g. [16]). This resonance was implicit in the shallow water analysis in [11] and here we give an explicit proof of the existence of the resonance and extend it to the finite depth model.

Cooker [11] showed that the natural frequencies in shallow water, for dynamic coupling between the vessel motion and an anti-symmetric fluid mode, are determined by the roots of $\mathrm{D}^{\mathrm{SW}}(s) = 0$ where

$$\mathrm{D}^{\mathrm{SW}}(s) = \frac{G}{s} - Rs - \tan s \,, \tag{1.2}$$

where s is the dimensionless natural frequency

$$s = \frac{\omega}{\sqrt{g h_0}} \frac{L}{2} \,, \tag{1.3}$$

and ω is the dimensional natural frequency. The dimensionless parameters G and R were first introduced in [11] and they are defined by

$$R = \frac{m_v}{m_f} \quad \text{and} \quad G = \frac{\nu L^2}{4 g h_0 m_f} \,, \tag{1.4}$$

where m_v is the mass of the dry vessel, and $m_f = \rho h_0 L$ is the mass of the fluid per unit width. The parameter ν is the spring stiffness parameter due to the gravitational restoring force,

$$\nu = \frac{g}{\ell}(m_f + m_v)\,. \tag{1.5}$$

The characteristic function (1.2) can not have a $1:1$ resonance since all the roots are simple. In fact there is a missing term in (1.2) [6]. The characteristic equation should be the product of two terms

$$\Delta^{\mathrm{SW}}(s) = \mathrm{P}^{\mathrm{SW}}(s)\,\mathrm{D}^{\mathrm{SW}}(s) \quad \text{with} \quad \mathrm{P}^{\mathrm{SW}}(s) = \sin(s)\,. \tag{1.6}$$

With the additional term there is an explicit $1:1$ resonance when both factors vanish simultaneously. This occurs precisely when G and R satisfy

$$G = s_m^2\, R\,, \quad \text{with } s_m = m\pi \text{ for any } m \in \mathbb{N}\,. \tag{1.7}$$

This observation makes explicit the resonance noted in [11]. A detailed analysis of the $1:1$ resonance in the shallow water case is given in the technical report [6].

We show in general that the characteristic function in all cases (the shallow water model [11, 3], the finite modal expansion [20], the cosine expansion [13], and the vertical eigenfunction expansion [28]) is the product of two functions

$$\Delta(s) = \mathrm{P}(s)\,\mathrm{D}(s)\,, \tag{1.8}$$

where s is the dimensionless frequency (1.3) in all cases. The roots of $\mathrm{D}(s) = 0$ are the modes which couple an anti-symmetric fluid mode with the vessel mode, and the roots of $\mathrm{P}(s) = 0$ are associated with the symmetric fluid modes.

The product structure of the characteristic equation (1.8) arises because the eigenvalue problem for the natural frequency has a block diagonal structure. An important consequence of this structure is that the eigenfunctions associated with the roots of $\mathrm{P} = 0$ are always linearly independent from the eigenfunctions associated with the roots of $\mathrm{D} = 0$. The product structure (1.8) has three principal solutions:

1. $\mathrm{D}(s) = 0$ but $\mathrm{D}'(s) \neq 0$ and $\mathrm{P}(s) \neq 0$: anti-symmetric fluid mode coupled to vessel motion.

2. $\mathrm{P}(s) = 0$ but $\mathrm{P}'(s) \neq 0$ and $\mathrm{D}(s) \neq 0$: symmetric fluid mode decoupled from vessel motion.

3. $\mathrm{D}(s) = 0$ and $\mathrm{P}(s) = 0$ but $\mathrm{D}'(s) \neq 0$ and $\mathrm{P}'(s) \neq 0$: internal $1:1$ resonance with a symmetric and anti-symmetric fluid mode coupled to the vessel motion.

The third condition is equivalent to $\Delta(s) = \Delta'(s) = 0$ which is the necessary condition for a $1:1$ resonance. The second class of solutions are symmetric modes which do not generate any coupling with the vessel motion. Figure 3 shows the first two mode shapes for the free oscillations of the fluid, and it apparent why the symmetric mode can generate free oscillations without affecting the vessel motion. The pressure is symmetric and so the force on the right vessel wall exactly balances that on the left.

It is important to emphasize that the resonance here is an *internal resonance* between normal modes: two linearly independent eigenfunctions corresponding to the same natural

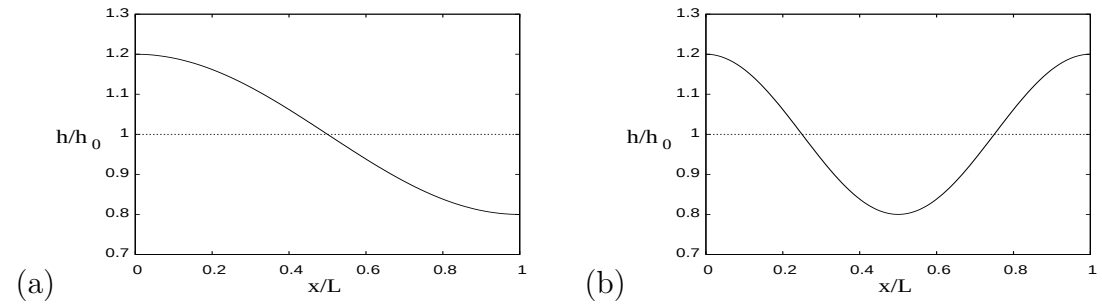

Figure 3: Mode shapes for the (a) first anti-symmetric and (b) first symmetric free oscillation modes

frequency. There is no forcing present. The theory of resonance due to external forcing requires different methods (e.g. Ockendon et al. [23, 24], Chapter 2 of [19]). Adding external forcing to an internal resonance would greatly enhance the range of response but external forcing is not considered in this paper. The internal resonances are of interest for two reasons: at the linear level it is a mechanism for excitation of symmetric fluid mode coupling to the vessel motion, and at the nonlinear level a $1:1$ resonance can give rise to much more dramatic fluid-vessel motion. A $1:1$ resonance in a different physical setting (Faraday experiment) is analyzed by [15, 16] and it gives some idea of the dramatic effect of the $1:1$ resonance in the weakly nonlinear problem. The effect of nonlinearity on the resonance is not considered in this paper (some comments on nonlinearity are in §8).

There are other potential internal resonances as well. For example the roots of either $\mathrm{P}(s)=0$ or $\mathrm{D}(s)=0$ may have modes with integer ratio, the most common of which is the $1:2$ resonance. For example in the case of free oscillations of the sloshing problem – with surface tension – it is shown by Vanden-Broeck [27] that a $1:2$ resonance occurs. A generalization of that $1:2$ resonance may also occur in modified form in the coupled problem if surface tension is added to the fluid. There is also the potential for rational ratios of any order: that is solutions of the form

$$\Delta(ms)=\Delta(ns)=0 \quad \text{for some natural numbers } (m,n)\,.$$

These higher-order resonances are not considered in this paper.

In this paper we extend all three classes of solutions identified above to the finite-depth model. When the depth is not small, the characteristic equation is much more complicated and will also depend on a third parameter: the depth ratio

$$\delta=\frac{h_0}{L}\,. \tag{1.9}$$

In this paper a new derivation of the coupled characteristic equation for finite depth is presented, using both the cosine expansion as in [13] and the vertical eigenfunction expansion as in [21, 28]. We find that the generalization of the shallow water resonance condition (1.7) is

$$\frac{G}{s_m}=Rs_m+s_m\sum_{n=1}^{\infty}\frac{c_n^2}{\frac{1}{2}k_nL}\tanh(\tfrac{1}{2}k_nL)\,. \tag{1.10}$$

with

$$s_m=m\pi\sqrt{\frac{\tanh\left(2m\pi\delta\right)}{2m\pi\delta}}\,,\quad \text{for any } m\in\mathbb{N}\,. \tag{1.11}$$

The various parameters in this expression are defined in §5.2. In the finite depth case, the range of physically-realizable values of parameters for the $1:1$ resonance is greatly extended. Both (1.7) and (1.10) are straight lines in the $(R,G)-$plane for each fixed m, but the slope for (1.7) is quite large whereas the slope decreases with increasing δ and becomes horizontal, and the $G-$intercept decreases, in the limit $\delta \to \infty$. Graphs illustrating the $\delta-$dependence of the resonance lines are presented in §7.4.

An outline of the paper is as follows. In §2 the nonlinear equations are summarized, with the details of the derivation of the vessel equation give in Appendix A. The linearized equations and the equations for the characteristic frequencies are derived in §2.1 to §2.3. The remainder of the paper is then the study of the time-harmonic solutions in order to determine the natural frequencies of the coupled problem. Section 4 presents the details of the cosine expansion approach to determining the characteristic equation and §5 presents the details using the vertical eigenfunction expansion. The explicit proof that the two representations are equivalent is given in §6.

Numerical for the non-resonant characteristic equation are presented in §7 and for the resonant case in §7.4. In the concluding remarks §8 some speculation on the implications of the $1:1$ resonance for the nonlinear problem is given.

2 Governing equations – finite depth model

The nonlinear equations for the fluid motion in Cooker's sloshing experiment are the Euler equations relative to a moving frame. Detailed derivations are given in [2] and [8]. The main new result is that the vessel motion is governed by the nonlinear pendulum equation forced by the fluid motion (1.1), and a derivation of that equation in given in Appendix A. The final form nonlinear equations with an irrotational velocity field are recorded here.

With a potential, ϕ, for the velocity field

$$u = \phi_x - \dot{q}_1 \quad \text{and} \quad v = \phi_y - \dot{q}_2\,, \tag{2.1}$$

where $q_1(t) = \ell \sin(\theta(t))$ and $q_2(t) = -\ell\cos(\theta(t))$, mass conservation gives

$$\Delta\phi := \phi_{xx} + \phi_{yy} = 0\,, \quad 0 < y < h(x,t)\,, \quad 0 < x < L\,. \tag{2.2}$$

Using the momentum equations to derive a Bernoulli equation, and then evaluating at the free surface gives the dynamic free surface boundary condition

$$\phi_t + \tfrac{1}{2}(\phi_x^2 + \phi_y^2) - \dot{q}_1\phi_x - \dot{q}_2\phi_y + gh + \tfrac{1}{2}(\dot{q}_1^2 + \dot{q}_2^2) = 0\,, \quad \text{at} \quad y = h(x,t)\,. \tag{2.3}$$

The kinematic free surface boundary condition is

$$h_t + (\phi_x - \dot{q}_1)h_x = \phi_y - \dot{q}_2 \quad \text{at} \quad y = h(x,t)\,. \tag{2.4}$$

The boundary conditions at the vessel walls are

$$\phi_y = \dot{q}_2 \quad \text{at} \quad y = 0 \quad \text{and} \quad \phi_x = \dot{q}_1 \quad \text{at} \quad x = 0, L\,. \tag{2.5}$$

For the vessel equation, with $(\mathscr{C}_1, \mathscr{C}_2)$ defined in Appendix A,

$$\mathscr{C}_1 = \sigma_1 - m_f\dot{q}_1\,, \quad \text{with} \quad \sigma_1 = \int_0^L \int_0^h \rho\phi_x \,\mathrm{d}y\mathrm{d}x\,,$$

and

$$\mathscr{C}_2 = \sigma_2 - m_f \dot{q}_2 \,, \quad \text{with} \quad \sigma_2 = \int_0^L \int_0^h \rho \phi_y \, \mathrm{d}y\mathrm{d}x \,.$$

Substitution into the vessel equation (A-2) gives

$$m_v \ddot{\theta} + \frac{g}{\ell}(m_v + m_f) \sin\theta = -\frac{1}{\ell} \cos\theta \dot{\sigma}_1 - \frac{1}{\ell} \sin\theta \dot{\sigma}_2 \,. \tag{2.6}$$

In summary, the governing equations for the nonlinear coupled problem with irrotational velocity field are $\Delta\phi = 0$ in the interior, the free surface boundary conditions (2.3)-(2.4), the bottom and side wall boundary conditions (2.5), and the vehicle equation (2.6).

2.1 Linear dynamically-coupled equations

The starting point for the linear analysis of the coupled problem, is obtained by linearizing the boundary conditions (2.3)-(2.4), (2.5), and the vehicle equation (2.6).

To leading order, the vessel velocity coordinates are approximated by $\dot{q}_1 \approx \ell\dot{\theta}$ and $\dot{q}_2 \approx 0$. The governing equation for ϕ in the linear approximation is still Laplace's equation

$$\phi_{xx} + \phi_{yy} = 0 \,, \quad 0 < y < h_0 \,, \quad 0 < x < L \,, \tag{2.7}$$

and the bottom and sidewall boundary conditions simplify to

$$\begin{aligned} \phi_y &= 0 \quad \text{at} \quad y = 0 \,, \\ \phi_x &= \ell\dot{\theta} \quad \text{at} \quad x = 0 \text{ and } x = L \,, \\ \phi_y &= h_t \quad \text{and} \quad \phi_t + gh = 0 \quad \Rightarrow \quad \phi_{tt} + g\phi_y = 0 \,, \quad \text{at } y = h_0 \,. \end{aligned} \tag{2.8}$$

The linearized vessel equation is

$$\frac{d}{dt}\left[\int_0^L \int_0^{h_0} \rho\phi_x \, \mathrm{d}y\mathrm{d}x + m_v \ell\dot{\theta}\right] + g(m_v + m_f)\theta = 0 \,. \tag{2.9}$$

2.2 Comparison with Frandsen's TLD model

To show that the linear equations (2.7)-(2.8) are equivalent to Frandsen's linearized TLD model, let

$$\phi(x, y, t) = \ell\dot{\theta}\, x + \Phi(x, y, t) \,,$$

and define $X(t) = \ell\theta(t)$. Then substitution into (2.7)-(2.8) gives a boundary value problem for $\Phi(x, y, t)$,

$$\Phi_{xx} + \Phi_{yy} = 0 \,, \quad 0 < y < h_0 \,, \quad 0 < x < L \,, \tag{2.10}$$

with boundary conditions

$$\begin{aligned} \Phi_y &= 0 \quad \text{at} \quad y = 0 \\ \Phi_x &= 0 \quad \text{at} \quad x = 0, L \,, \\ g\Phi_y &= -\Phi_{tt} - x\dddot{X} \quad \text{at} \quad y = h_0 \,. \end{aligned} \tag{2.11}$$

The linearized vessel equation is

$$(m_v + m_f)\ddot{X} + \nu X = -\int_0^L \int_0^{h_0} \rho \Phi_{xt} \, \mathrm{d}y \mathrm{d}x = \int_0^{h_0} \rho \Phi_t \, \mathrm{d}y \Big|_{x=L}^{x=0}, \tag{2.12}$$

with ν defined in (1.5). These equations for Φ are precisely equations (2.6) for ϕ on page 312 of [13], with the appropriate change of notation, and setting the damping coefficient c and the forcing function $F(t)$ to zero. In summary, the linear equations for the TLD model in [13] and [20] are exactly equivalent to the linearized equations for Cooker's sloshing experiment.

2.3 Natural frequencies of the linear coupled problem

To determine the natural frequencies of the linearized coupled problem, express ϕ, h and θ as time-periodic functions with frequency ω,

$$\phi = \widehat{\phi} \cos \omega t \,, \quad h = \widehat{h} \sin \omega t \,, \quad \theta = \widehat{\theta} \sin \omega t \,. \tag{2.13}$$

Then

$$\widehat{h} = \frac{\omega}{g} \widehat{\phi} \Big|^{y=h_0}, \tag{2.14}$$

and $\widehat{\phi}$ and $\widehat{\theta}$ satisfy the boundary value problem

$$\widehat{\phi}_{xx} + \widehat{\phi}_{yy} = 0 \,, \quad 0 < y < h_0 \,, \quad 0 < x < L \,, \tag{2.15}$$

with boundary conditions

$$\begin{aligned} \widehat{\phi}_y &= 0 \quad \text{at} \quad y = 0 \,, \\ \widehat{\phi}_y &= \tfrac{\omega^2}{g} \widehat{\phi} \quad \text{at} \quad y = h_0 \,, \\ \widehat{\phi}_x &= \ell \omega \widehat{\theta} \quad \text{at} \quad x = 0, L \,, \end{aligned} \tag{2.16}$$

and vessel equation

$$\left(\frac{g(m_v + m_f)}{\omega} - m_v \ell \omega \right) \widehat{\theta} = \int_0^L \int_0^{h_0} \rho \widehat{\phi}_x \, \mathrm{d}y \mathrm{d}x \,. \tag{2.17}$$

The coupled equations (2.15)-(2.17) form an eigenvalue problem for the natural frequency ω of the coupled problem. The equation (2.15) with the boundary conditions (2.16) is well studied in the case where $\theta(t)$ is given – the forced problem (see §2.2.2 of [21] and §2.6 of [19]). In the coupled problem, an additional equation (2.17) has to be solved for the vessel motion.

3 Method 1: finite modal expansion

The first approach proposed for the coupled linear finite depth problem (2.7)-(2.9) was a finite modal expansion by Ikeda & Nakagawa [20]. They expressed the fluid motion in terms of the first anti-symmetric and first symmetric fluid mode, coupled to the vessel

motion (see equation (15) in [20]). Their motivation was to study the nonlinear problem by modelling it with 3 coupled nonlinear ODEs. However, for the purposes of this paper we review the linear version of their modal expansion as it provides a simplified model of the full infinite expansion considered in §4, and has the three principal solutions in simplified form.

Consider the three term approximation

$$\phi(x,y,t) = \dot{X}(t)\left(x - \tfrac{1}{2}L\right) + a_0(t)\frac{\cosh(\alpha_0 y)}{\cosh(\alpha_0 h_0)}\cos(\alpha_0 x) + b_1(t)\frac{\cosh(\beta_1 y)}{\cosh(\beta_1 h_0)}\cos(\beta_1 x)\,, \quad (3.1)$$

where $X(t) = \ell\theta(t)$, $\alpha_0 = \pi/L$ and $\beta_1 = 2\pi/L$. Substitution into the boundary conditions (2.8) and vessel equation (2.9) gives the three coupled equations

$$\begin{aligned} \ddot{b}_1 + g\beta_1 \tanh(\beta_1 h_0)\, b_1 &= 0 \\ \ddot{a}_0 + g\alpha_0 \tanh(\alpha_0 h_0)\, a_0 &= \frac{4}{L\alpha_0^2}\dddot{X} \\ (m_v + m_f)\ddot{X} + \nu X &= \frac{2\rho}{\alpha_0}\tanh(\alpha_0 h_0)\,\dot{a}_0\,. \end{aligned} \quad (3.2)$$

With appropriate change of notation, these are the linear parts of equations (18a)-(18e) in [20]. The second and third equations are equivalent to equations (20)-(21) in [20]. The notation (a_1, a_2, x_1) there corresponds to (a_0, b_1, X) here. The first equation in (3.2) is dropped from the linear analysis in [20]. All three modes are retained here.

Look for time-periodic solutions of frequency ω,

$$X(t) = \widehat{X}\,\sin(\omega t)\,, \quad a_0(t) = \widehat{a_0}\,\cos(\omega t) \quad \text{and} \quad b_1(t) = \widehat{b_1}\,\cos(\omega t)\,.$$

Substitution into (3.2) reduces the ODEs to a homogeneous matrix equation

$$\begin{bmatrix} -\omega^2 + g\beta_1\tanh(\beta_1 h_0) & 0 & 0 \\ 0 & -\omega^2 + g\alpha_0\tanh(\alpha_0 h_0) & \frac{4}{L\alpha_0^2}\omega^3 \\ 0 & \frac{2\rho}{\alpha_0}\omega\tanh(\alpha_0 h_0) & -(m_v+m_f)\omega^2 + \nu \end{bmatrix} \begin{pmatrix} \widehat{b_1} \\ \widehat{a_0} \\ \widehat{X} \end{pmatrix} = \begin{pmatrix} 0 \\ 0 \\ 0 \end{pmatrix}. \quad (3.3)$$

Vanishing of the determinant of the coefficient matrix then gives the characteristic equation $\Delta^{\rm IN}(\omega) = 0$ with

$$\Delta^{\rm IN}(\omega) = {\rm P}^{\rm IN}(\omega){\rm D}^{\rm IN}(\omega)\,, \quad (3.4)$$

where

$${\rm P}^{\rm IN}(\omega) = -\omega^2 + g\beta_1\tanh(\beta_1 h_0)\,, \quad (3.5)$$

and

$${\rm D}^{\rm IN}(\omega) = \big(-\omega^2 + g\alpha_0\tanh(\alpha_0 h_0)\big)\big(-(m_v+m_f)\omega^2 + \nu\big) - \frac{8\rho}{L\alpha_0^3}\omega^4\tanh(\alpha_0 h_0)\,. \quad (3.6)$$

The decoupling of the b_1 mode is reflected in the block diagonal structure of the coefficient matrix in (3.3). As a consequence, the eigenvector associated with the b_1 mode is linearly independent from any of the eigenvectors of the other modes. A fact which is important for the internal $1:1$ resonance.

The conditions for the first class of solutions are

$$\mathrm{D}^{\mathrm{IN}}(\omega) = 0 \quad \text{and} \quad \mathrm{P}^{\mathrm{IN}}(\omega) \neq 0\,.$$

This class of solutions is the one considered in [20]: see equation (23) in [20] where the two roots of $\mathrm{D}^{\mathrm{IN}}(\omega) = 0$ are labelled q_1^2 and q_2^2. These modes consist of an anti-symmetric fluid mode coupled to the vessel motion.

The conditions for the second class of solutions are

$$\mathrm{P}^{\mathrm{IN}}(\omega) = 0 \quad \text{and} \quad \mathrm{D}^{\mathrm{IN}}(\omega) \neq 0\,.$$

With s as in (1.3), the condition $\mathrm{P}^{\mathrm{IN}}(\omega) = 0$ gives

$$s^2 = \pi^2 \frac{\tanh(2\pi\delta)}{2\pi\delta}\,.$$

Since $\mathrm{D}^{\mathrm{IN}}(\omega) \neq 0$, it follows that $\widehat{a_0} = X = 0$ but $\widehat{b_1} \neq 0$ and so the mode is a symmetric fluid motion uncoupled from the vehicle motion.

3.1 1:1 resonance in the finite mode case

Since the third class of solutions requires both $\mathrm{D}^{\mathrm{IN}} = \mathrm{P}^{\mathrm{IN}} = 0$ to vanish it puts a constraint on parameter space. For comparison with other methods in this paper, first put the factors in (3.4) into dimensionless form using (1.3) and (1.4),

$$\begin{aligned} \mathrm{P}^{\mathrm{IN}}(s) &= -s^2 + \pi^2 \frac{\tanh(\beta_1 h_0)}{\beta_1 h_0} \\ \mathrm{D}^{\mathrm{IN}}(s) &= \big[-s^2 + (\tfrac{1}{2}\alpha_0 L)^2 \mathcal{T}_0\big]\big[G - (1+R)s^2\big] - \frac{8\mathcal{T}_0}{(\alpha_0 L)^2} s^4\,, \end{aligned} \tag{3.7}$$

with

$$\mathcal{T}_0 := \frac{\tanh(\alpha_0 h_0)}{\alpha_0 h_0}\,. \tag{3.8}$$

Now substitute the solution of $\mathrm{P}^{\mathrm{IN}}(s) = 0$,

$$s_0 = \pi \sqrt{\frac{\tanh(\beta_1 h_0)}{\beta_1 h_0}}\,, \tag{3.9}$$

into $\mathrm{D}^{\mathrm{IN}}(s) = 0$ giving, after some rearrangement,

$$\frac{G}{s_0} - R s_0 = s_0 + \frac{8\mathcal{T}_0}{(\alpha_0 L)^2} \frac{s_0^3}{(\tfrac{1}{2}\alpha_0 L)^2 \mathcal{T}_0 - s_0^2}\,. \tag{3.10}$$

This condition is the analogue of the condition (1.7) for the shallow water model and the analogue of the condition (1.10) for the finite-depth model. It gives a $\delta-$dependent straight line in the $(R, G)-$plane by noting that $\alpha_0 h_0 = L\alpha_0\delta$ in dimensionless form.

To compare with (1.7) take the limit $\delta \to 0$ giving $\mathcal{T}_0 = 1$ and $s_0 = \pi$ and so

$$G = \pi^2 R + \pi^2 - \frac{32}{3}\,, \tag{3.11}$$

which has the same slope as the line in (1.7) but with a slightly lower value of the $G-$intercept.

For finite δ, it is not obvious that (3.10) is related to the exact finite depth condition (1.10). However, it is related, and the relationship between the two is easier to see once the infinite cosine expansion is introduced and is therefore considered in §4.

The resonance (3.10) is not considered in [20]. However, they consider two other forms of resonance. The first resonance considered in [20] is a resonance between the dry vessel ($\sqrt{k/Q_{17}}$ in the notation there) and the *first anti-symmetric mode* (see discussion in the beginning of §3 on page 31 of [20]). They also bring in a second form of resonance by introducing a forcing function, and then a resonance can be introduced by choosing the forcing frequency near one of the system frequencies. The principal aim in [20] is to study the effect of nonlinearity.

4 Method 2: an infinite cosine expansion

In the absence of the coupling equation, the linear problem (2.15)-(2.16) is equivalent to the problem of forced oscillations with $\theta(t)$ specified. This problem was first considered by Graham & Rodriguez [17] (see also §2.6.1 of [19] and §5.2 of [12]). Their strategy for solving (2.15)-(2.16) is to transform $\widehat{\phi}$ so that the inhomogeneous boundary conditions at $x = 0, L$ are moved to $y = h_0$. Then a cosine expansion in the $x-$direction can be used. Let

$$\widehat{\phi}(x,y) = \ell\omega\widehat{\theta}\left(x - \tfrac{1}{2}L\right) + \widehat{\Phi}(x,y)\,. \tag{4.1}$$

The function $\widehat{\Phi}(x,y)$ then satisfies Laplace's equation and the boundary conditions

$$\widehat{\Phi}_y = \frac{\omega^2}{g}\widehat{\Phi} + \ell\widehat{\theta}\frac{\omega^3}{g}\left(x - \tfrac{1}{2}L\right)\,, \quad y = h_0\,, \tag{4.2}$$

$$\widehat{\Phi}_y = 0\,, \quad y = 0\,, \tag{4.3}$$

$$\widehat{\Phi}_x = 0\,, \quad x = 0, L\,. \tag{4.4}$$

The inhomogeneous term at $y = h_0$ has the following cosine expansion

$$x - \frac{L}{2} = \sum_{n=0}^{\infty} p_n \cos(\alpha_n x) = -\frac{4}{L}\sum_{n=0}^{\infty}\frac{1}{\alpha_n^2}\cos(\alpha_n x)\,, \quad \alpha_n = (2n+1)\frac{\pi}{L}\,. \tag{4.5}$$

This form of the boundary condition suggests that the following form for the $\widehat{\Phi}$ solution

$$\widehat{\Phi}(x,y) = \sum_{n=1}^{\infty} b_n \frac{\cosh(\beta_n y)}{\cosh(\beta_n h_0)}\cos(\beta_n x) + \sum_{n=0}^{\infty} a_n \frac{\cosh(\alpha_n y)}{\cosh(\alpha_n h_0)}\cos(\alpha_n x)\,, \tag{4.6}$$

where $\beta_n = 2n\pi/L$. The first term gives the homogeneous solution and the second term gives the particular solution associated with the $\widehat{\theta}$ term in (4.2). The coefficients a_n and b_n are determined by substitution into the boundary condition at $y = h_0$, giving

$$\left(\beta_n \tanh(\beta_n h_0) - \frac{\omega^2}{g}\right) b_n = 0\,, \tag{4.7}$$

and

$$\left(\alpha_n \tanh(\alpha_n h_0) - \frac{\omega^2}{g}\right) a_n = -\ell\omega\widehat{\theta}\,\frac{4}{L\alpha_n^2}\frac{\omega^2}{g}\,. \tag{4.8}$$

This completes the solution of the forced problem. Now substitute the general form for $\widehat{\phi}(x,y)$ in (4.1) into the coupling equation for $\widehat{\theta}$,

$$(m_v + m_f)\left(\frac{g}{\omega} - \ell\omega\right)\widehat{\theta} = \int_0^L \int_0^{h_0} \rho\widehat{\Phi}_x \,\mathrm{d}y\mathrm{d}x\,,$$

or

$$(m_v + m_f)\left(\frac{g}{\omega} - \ell\omega\right)\widehat{\theta} = -2\rho\sum_{n=0}^{\infty}\frac{a_n}{\alpha_n}\,\tanh(\alpha_n h_0)\,. \tag{4.9}$$

The three equations (4.7)-(4.9) are three homogeneous equations for the unknowns $\widehat{\theta}$, $a_0, a_1, \ldots$, and $b_1, b_2, \cdots$. The first equation (4.7) is homogeneous, diagonal and decouples from the other equations. Its characteristic function is

$$\mathrm{P}^{\cos}(\omega) = \prod_{m=1}^{\infty}\left(\omega^2 - g\beta_m \tanh(\beta_m h_0)\right). \tag{4.10}$$

The complete characteristic function is

$$\Delta^{\cos}(\omega) = \mathrm{P}^{\cos}(\omega)\mathrm{D}^{\cos}(\omega)\,. \tag{4.11}$$

Now derive the characteristic function $\mathrm{D}^{\cos}$ for the coupled modes. It is this characteristic equation which was first studied in [13]. Set $b_n = 0$ for all n and assume $\widehat{\theta} \neq 0$. Then (4.8) can be solved for a_n and substituted into (4.6)

$$\widehat{\Phi}(x,y) = -\ell\omega\widehat{\theta}\,\frac{4\omega^2}{Lg}\sum_{n=0}^{\infty}\frac{(\alpha_n\tanh(\alpha_n h_0) - \omega^2/g)^{-1}}{\alpha_n^2}\,\frac{\cosh(\alpha_n y)}{\cosh(\alpha_n h_0)}\cos(\alpha_n x)\,. \tag{4.12}$$

Substitution into the coupling equation (4.9) then gives $\mathrm{D}^{\cos}(\omega) = 0$ with

$$\mathrm{D}^{\cos}(\omega) = \left[(m_v + m_f)\left(\frac{g}{\omega} - \ell\omega\right) - \frac{8\ell m_f}{L^2 h_0}\frac{\omega^3}{g}\sum_{n=0}^{\infty}\frac{1}{\alpha_n^3}\frac{\tanh(\alpha_n h_0)}{\left(\alpha_n\tanh(\alpha_n h_0) - \frac{\omega^2}{g}\right)}\right]. \tag{4.13}$$

This characteristic equation is implicit in [13]. The strategy there is to use an infinite determinant expansion resulting in a product formula (see equation (4.1) in [13]).

Here the explicit form (4.13) will be used. Exact solutions are still impossible, but the explicit form is useful for numerical computation of the frequencies. First transform (4.13) to dimensionless form. Let

$$\gamma_n = (2n+1)\pi \quad \text{and} \quad T_n = \tanh(\alpha_n h_0) = \tanh(\gamma_n \delta)\,.$$

Then, using the Cooker parameters (1.4), dividing by $\omega m_f L$, noting that

$$\frac{\ell}{L} = \frac{1}{4\delta}\frac{(1+R)}{G}\,,$$

replacing ω with s in (1.3), and multiplying by s,

$$\mathrm{D}^{\cos}(s) = \frac{G}{s} - (1+R)s - 32s^3 \sum_{n=0}^{\infty} \frac{1}{\gamma_n^3} \frac{T_n}{\left(\gamma_n T_n - 4\delta s^2\right)}\,, \tag{4.14}$$

where for brevity the same symbol, $\mathrm{D}^{\cos}$, is used for the dimensionless characteristic function (4.14). The complete characteristic function in dimensionless form is the product

$$\Delta^{\cos}(s) = \mathrm{P}^{\cos}(s)\,\mathrm{D}^{\cos}(s)\,, \tag{4.15}$$

with $\mathrm{P}^{\cos}(s)$ the dimensionless form of (4.10),

$$\mathrm{P}^{\cos}(s) = \prod_{m=1}^{\infty} \left(s^2 - m^2\pi^2 \frac{\tanh(2m\pi\delta)}{2m\pi\delta} \right). \tag{4.16}$$

Setting $\mathrm{D}^{\cos}(s) = 0$ with $\mathrm{P}^{\cos}(s) \neq 0$ gives the non-resonant coupling between the vessel motion and an anti-symmetric fluid mode. Setting $\mathrm{P}^{\cos}(s) = 0$ with $\mathrm{D}^{\cos}(s) \neq 0$ gives a symmetric fluid mode, decoupled from the vessel motion.

4.1 1:1 resonance in the cosine formulation

The $1:1$ resonance in the cosine formulation is obtained by setting the two factors in (4.15) to zero simultaneously. Setting the first factor to zero amounts to choosing a symmetric fluid mode; that is, for some $m \in \mathbb{N}$, $b_m \neq 0$ and $b_n = 0$ for all $n \neq m$, and

$$\omega_m^2 = g\beta_m \tanh(\beta_m h_0)\,.$$

In dimensionless form,

$$s_m = m\pi \sqrt{\frac{\tanh(2m\pi\delta)}{2m\pi\delta}}\,. \tag{4.17}$$

The expression for a_n in (4.8) then becomes

$$a_n = -4\frac{\ell}{L}\omega\widehat{\theta}\frac{s_m^2}{\alpha_n^2}\frac{1}{\sigma_{m,n}}\,, \tag{4.18}$$

where

$$\sigma_{m,n} = \left[\frac{(2n+1)}{2}\pi\right]^2 \frac{\tanh(\alpha_n h_0)}{\alpha_n h_0} - s_m^2\,.$$

Substitution into (4.9) and scaling gives

$$\left[\frac{G}{s_m^2} - R - 1 - \frac{8}{\delta}s_m^2 \sum_{n=0}^{\infty} \frac{\tanh(\alpha_n h_0)}{(\alpha_n L)^3 \sigma_{m,n}}\right]\widehat{\theta} = 0\,. \tag{4.19}$$

Since we are interested in coupled modes, divide by $\widehat{\theta}$. Then there is a line in the $(R,G)-$plane where a resonance between the vessel motion and the symmetric mode exists,

$$G = s_m^2 R + s_m^2 + \frac{8}{\delta}s_m^4 \sum_{n=0}^{\infty} \frac{\tanh((2n+1)\pi\delta)}{(2n+1)^3\pi^3\,\sigma_{m,n}}\,. \tag{4.20}$$

This expression is the analogue of (1.10). It is not obvious that they are equivalent. Using an explicit transformation it is proved in §6 that (4.20) and (1.10) are equivalent.

To show that the resonance line (4.20) reduces to the resonance line in the Ikeda-Nakagawa formulation (3.10) truncate the sum to the first term in (4.20) and take $s_m = s_0$, where s_0 is defined in (3.9),

$$\frac{G}{s_0} - s_0 R = s_0 + \frac{8}{\delta} s_0^3 \frac{\tanh(\pi\delta)}{\pi^3\, \sigma_{0,0}} = s_0 + 8 s_0^3 \frac{\mathcal{T}_0}{\pi^2\, (\frac{1}{4}\pi^2 \mathcal{T}_0 - s_0^2)}\,,$$

which agrees with (3.10), noting that $\alpha_0 L = \pi$.

We will show in §6 that the representation of the eigenfunctions is equivalent in the cosine and vertical eigenfunction expansions and therefore the eigenfunctions in the resonance case will be discussed in §5.

5 Method 3: vertical eigenfunction expansion

Another approach to computing the natural frequencies is to use a *vertical eigenfunction expansion*. This strategy is suggested in §2.1 of Linton & McIver [21], and is used there to solve the forced problem (see §2.2.2 in [21]); that is, (2.15)-(2.16) with $\theta(t)$ considered as given. The boundary value problem (2.15)-(2.16) is solved using the eigenfunction expansion,

$$\widehat{\phi}(x,y) = \sum_{n=0}^{\infty} A_n(x)\psi_n(y)\,, \tag{5.1}$$

where the vertical eigenfunctions satisfy the eigenvalue problem

$$\begin{aligned} -\psi_{yy} &= \lambda\psi\,, \quad 0 < y < h_0\,, \\ \psi_y &= 0 \quad \text{at } y = 0 \quad \text{and} \quad \psi_y = \tfrac{\omega^2}{g}\psi \quad \text{at } y = h_0\,. \end{aligned} \tag{5.2}$$

For given ω this boundary value problem has an infinite number of eigenvalues λ_n, and the associated eigenfunctions form a complete set. The first eigenvalue is negative, $\lambda_0 = -k_0^2$ and the rest are positive, $\lambda_n = k_n^2$, $n = 1, 2, \ldots$. The first eigenfunction $\psi_0(y)$ is associated with the *wave mode* and the eigenfunctions $\psi_n(y)$, $n = 1, 2, \ldots$, are associated with the *evanescent modes*. The other properties of the eigenfunctions needed here are recorded in Appendix B.

Laplace's equation and the properties of the eigenfunctions give

$$\begin{aligned} A_0(x) &= A_0^{(1)} \cos k_0 x + A_0^{(2)} \sin k_0 x \\ A_n(x) &= A_n^{(1)} \cosh k_n x + A_n^{(2)} \sinh k_n x\,, \quad n = 1, 2, \ldots\,. \end{aligned} \tag{5.3}$$

The coefficients are determined by imposing the boundary conditions at $x = 0$ and $x = L$

$$A_n'(0) = A_n'(L) = \ell\omega\widehat{\theta}\, c_n\,, \quad n = 0, 1, \cdots\,, \tag{5.4}$$

where the expansion $1 = \sum_{n=0}^{\infty} c_n \psi_n(y)$ is used. The coefficients (using (B-9) in Appendix B) are

$$c_0 = \frac{1}{N_0} \frac{\sinh(k_0 h_0)}{k_0 h_0} \quad \text{and} \quad c_n = \frac{1}{N_n} \frac{\sin(k_n h_0)}{k_n h_0}\,.$$

The critical equations in the set (5.4) are the ones for $n = 0$ since they contain information associated with the resonance. The condition (5.4) with $n = 0$ gives

$$A_0^{(2)} = \frac{1}{k_0}\ell\omega\widehat{\theta}c_0\,.$$

The condition at $x = L$ and $n = 0$ requires

$$-2k_0A_0^{(1)}\sin\tfrac{1}{2}k_0L\cos\tfrac{1}{2}k_0L = 2\ell\omega\widehat{\theta}c_0(\sin^2\tfrac{1}{2}k_0L)\,.$$

At this point there is a temptation to impose the assumption

$$\sin\left(\tfrac{1}{2}k_0L\right) \neq 0\,. \tag{5.5}$$

If this assumption is imposed then

$$A_0^{(1)} = -\frac{c_0}{k_0}\tan\left(\tfrac{1}{2}k_0L\right)\ell\omega\widehat{\theta}\,. \tag{5.6}$$

In this case the wave mode ($n = 0$) is intrinsically coupled to the evanescent modes ($n \geq 1$). However, this assumption rules out important resonant solutions (cf. §5.2).

Hence the strategy at this point is to leave both parameters $A_0^{(1)}$ and $\widehat{\theta}$ free with the relation

$$k_0\sin(k_0L)\,A_0^{(1)} + \ell\omega\widehat{\theta}c_0(1-\cos k_0L) = 0\,, \tag{5.7}$$

and $A_0(x)$ is left in the general form

$$A_0(x) = A_0^{(1)}\cos k_0x + \frac{1}{k_0}\ell\omega\widehat{\theta}c_0\sin k_0x\,. \tag{5.8}$$

Solving the systems (5.4) for $n \geq 1$ is much simpler as there are no singularities. Solving these equations for the coefficients $A_n^{(1)}$ and $A_n^{(2)}$ results in

$$A_n(x) = \ell\omega\widehat{\theta}\frac{c_n}{k_n}\left(\sinh(k_nx) - \tanh(\tfrac{1}{2}k_nL)\,\cosh(k_nx)\right)\,. \tag{5.9}$$

In this case there is no additional assumption like (5.5) required, since

$$\sinh\left(\tfrac{1}{2}k_nL\right) \neq 0 \quad \text{for all} \quad n \geq 1\,. \tag{5.10}$$

The evanescent modes (5.9) are proportional to $\widehat{\theta}$ and so are intrinsically coupled to the vessel motion.

This completes the construction of the function $\widehat{\phi}(x,y)$ satisfying $\Delta\widehat{\phi} = 0$ and the three boundary conditions (2.16). This solution agrees with the expression for the potential in (2.29) in §2.2.2 of [21].

5.1 Coupling between $\widehat{\theta}$ and $\widehat{\phi}$

Substituting the expansion for $\widehat{\phi}$ into the coupling equation (2.17) gives

$$\begin{aligned}\left(\frac{g(m_v+m_f)}{\omega} - m_v\ell\omega\right)\widehat{\theta} \;&=\; \rho c_0h_0A_0^{(1)}(\cos(k_0L)-1) + \rho h_0\frac{\ell}{k_0}\omega c_0^2\sin(k_0L)\widehat{\theta} \\ &\quad +2\rho h_0\ell\omega\widehat{\theta}\sum_{n=1}^{\infty}\frac{c_n^2}{k_n}\tanh(\tfrac{1}{2}k_nL)\,.\end{aligned} \tag{5.11}$$

The two equations (5.7) and (5.11) are two homogeneous equations for the two unknowns $A_0^{(1)}$ and $\widehat{\theta}$. They can be expressed in matrix form

$$\begin{bmatrix} k_0 \sin(k_0 L) & (1-\cos(k_0 L))\ell\omega c_0 \\ \rho c_0 h_0(\cos(k_0 L)-1) & \Theta \end{bmatrix} \begin{pmatrix} A_0^{(1)} \\ \widehat{\theta} \end{pmatrix} = \begin{pmatrix} 0 \\ 0 \end{pmatrix}, \tag{5.12}$$

where

$$\Theta := \rho \frac{h_0}{k_0} \ell\omega c_0^2 \sin(k_0 L) - \left(\frac{g(m_v+m_f)}{\omega} - m_v \ell\omega \right) + 2\rho h_0 \ell\omega \sum_{n=1}^{\infty} \frac{c_n^2}{k_n} \tanh(\tfrac{1}{2} k_n L) \,. \tag{5.13}$$

The homogeneous equation (5.12) has a solution if and only if the determinant of the coefficient matrix vanishes. This condition provides the characteristic equation $\Delta^{\text{vert}}(\omega) = 0$ where

$$\Delta^{\text{vert}}(\omega) = \det \begin{bmatrix} k_0 \sin(k_0 L) & (1-\cos(k_0 L))\ell\omega c_0 \\ \rho c_0 h_0(\cos(k_0 L)-1) & \Theta \end{bmatrix},$$

or

$$\Delta^{\text{vert}} = k_0 \sin(k_0 L)\Theta + \rho h_0 \ell\omega c_0^2 (1-\cos(k_0 L))^2 \,.$$

After some algebra, this expression can be written in the form

$$\Delta^{\text{vert}}(\omega) = 2k_0 \sin\left(\tfrac{1}{2} k_0 L\right) \cos(\tfrac{1}{2} k_0 L)\, \mathrm{D}^{\text{vert}}(\omega) \,,$$

with

$$\begin{aligned} \mathrm{D}^{\text{vert}}(\omega) \;\; = \;\; & -\left(\frac{g(m_v+m_f)}{\omega} - m_v \ell\omega \right) + 2\rho \frac{h_0}{k_0} \ell\omega c_0^2 \tan(\tfrac{1}{2} k_0 L) \\ & + 2\rho h_0 \ell\omega \sum_{n=1}^{\infty} \frac{c_n^2}{k_n} \tanh(\tfrac{1}{2} k_n L) \,. \end{aligned} \tag{5.14}$$

The factor $k_0 \cos\left(\frac{1}{2} k_0 L\right)$ is never zero. This property follows by noting that $k_0 = 0$ is not a solution of the characteristic equation (B-3) for $\omega \neq 0$ and the product $\cos\left(\frac{1}{2} k_0 L\right) \mathrm{D}^{\text{vert}}$ is strictly positive when $\frac{1}{2} k_0 L$ is an odd multiple of $\frac{1}{2}\pi$. Hence the appropriate characteristic equation is $\Delta^{\text{vert}}(\omega) = 0$ where

$$\Delta^{\text{vert}}(\omega) = \mathrm{P}^{\text{vert}}(\omega)\, \mathrm{D}^{\text{vert}}(\omega) \,, \quad \text{with} \quad \mathrm{P}^{\text{vert}}(\omega) := \sin\left(\tfrac{1}{2} k_0 L\right). \tag{5.15}$$

The characteristic function is a bit easier to interpret if it is made dimensionless. Introduce the scaling (1.4) into (5.14) and divide by $-2m_f \ell L^{-1}\sqrt{g h_0}$,

$$\mathrm{D}^{\text{vert}}(s) = \left(\frac{G}{s} - Rs \right) - s \frac{2c_0^2}{k_0 L} \tan(\tfrac{1}{2} k_0 L) - s \sum_{n=1}^{\infty} \frac{2c_n^2}{k_n L} \tanh(\tfrac{1}{2} k_n L) \,, \tag{5.16}$$

where for brevity the same symbol D^{vert} is used.

The factor D^{vert} in (5.16) agrees with the result derived by Yu [28]. The derivation in [28] implicitly uses a vertical eigenfunction expansion. By translating the notation in [28] to the notation here it can be shown that the expression for the characteristic equation in [28] agrees with D^{vert}. However, the characteristic equation in [28] is missing the factor $\sin(\frac{1}{2} k_0(s) L)$ in (5.15).

The complete dimensionless characteristic equation is $\Delta^{\rm vert}(s) = 0$ where

$$\Delta^{\rm vert}(s) = {\rm P}^{\rm vert}(s)\,{\rm D}^{\rm vert}(s)\,, \quad \text{with} \quad {\rm P}^{\rm vert}(s) := \sin\left(\tfrac{1}{2}\,k_0(s)L\right), \tag{5.17}$$

with ${\rm D}^{\rm vert}(s)$ defined in (5.16). It is remarkable that the two representations of the characteristic equation (5.16) and (4.14) are exactly the same. A proof of this equivalence is given in §6.

5.2 1:1 resonance in the vertical eigenfunction representation

The $1:1$ resonance occurs when the two factors in the product representation (5.17) vanish simultaneously,

$${\rm P}^{\rm vert}(s) = 0 \quad \text{and} \quad {\rm D}^{\rm vert}(s) = 0\,. \tag{5.18}$$

Vanishing of the first factor gives

$$k_0 L = 2m\pi \quad \text{for any integer } m\,. \tag{5.19}$$

Using (B-3), the value of s is

$$s_m = m\pi\sqrt{\frac{\tanh\left(2m\pi\delta\right)}{2m\pi\delta}}\,. \tag{5.20}$$

This sequence of values of s is associated with symmetric sloshing modes.

With the condition (5.19) the equation (5.7) is exactly satisfied. The second equation (5.11) is equivalent to the the vanishing of the second factor in (5.18). With $\widehat{\theta} \neq 0$, the required condition is

$$\frac{G}{s} = Rs + s\sum_{n=1}^{\infty}\frac{c_n^2}{\frac{1}{2}\,k_n L}\tanh(\tfrac{1}{2}\,k_n L)\,. \tag{5.21}$$

In this equation s is fixed by the choice of m in (5.20) and this choice in turn determines the values of k_n for $n \geq 1$ via

$$k_n^2 L^2\frac{\tan(\delta k_n L)}{\delta k_n L} = -4m^2\pi^2\frac{\tanh\left(2m\pi\delta\right)}{2m\pi\delta}\,.$$

Hence for fixed m in (5.19) and fixed δ the condition (5.21) gives a line in the (R, G) plane along which there is a resonance. Calculations for a range of δ values are shown in Figure 4. In all cases the resonance curve is a straight line. In the limit of shallow water it has a steep slope and passes through the origin. As δ increases the slope decreases and the $G-$intercept increases, to the point where the line is almost horizontal in the limit of deep water. As δ ranges from shallow water to deep water, a dense region of the (R, G) parameter space is covered.

5.3 The eigenfunctions at resonance

At resonance, there are two linearly independent eigenfunctions parameterized by $A_0^{(1)}$ and $\widehat{\theta}$. The eigenfunctions for $\theta(t)$ and $\phi(x, y, t)$ for each m are

$$\begin{aligned} \theta_m(t) &= \widehat{\theta}\sin(\omega_m t), \\ \phi_m(x, y, t) &= \widehat{\phi}(x, y)\cos(\omega_m t)\,, \end{aligned} \tag{5.22}$$

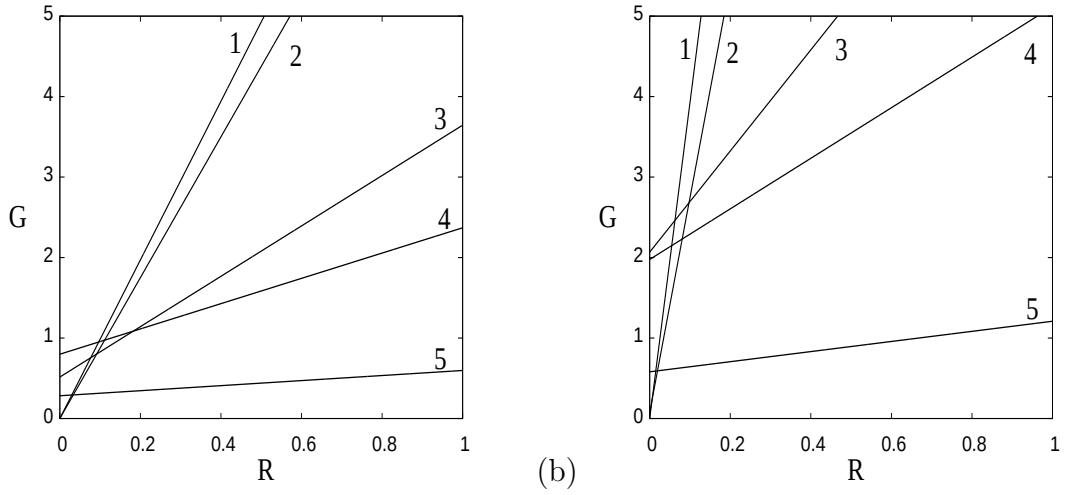

Figure 4: Plot of the (a) the first ($m = 1$) and (b) the second ($m = 2$) resonance curve in the $(G, R)-$plane, for $\delta = 0.01,\ 0.1,\ 0.5,\ 1.0$ and 5.0 numbered $1 - 5$ respectively.

with $\omega_m = \frac{2}{L}\sqrt{gh_0}s_m$, and $\widehat{\phi}(x,y) = \sum_{n=0}^{\infty} A_n(x)\psi_n(y)$. Now separate $\widehat{\phi}$ into two parts, one proportional to $A_0^{(1)}$ and the other proportional to $\widehat{\theta}$,

$$\widehat{\phi}(x,y) = A_0^{(1)}\widehat{\phi}_1^{\text{vert}}(x,y) + \ell\omega\widehat{\theta}\,\widehat{\phi}_2^{\text{vert}}(x,y)\,,$$

with

$$\widehat{\phi}_1^{\text{vert}}(x,y) = \cos(k_0 x)\psi_0(y), \tag{5.23}$$

and

$$\widehat{\phi}_2^{\text{vert}}(x,y) = \frac{c_0}{k_0}\sin(k_0 x)\,\psi_0(y) + \sum_{n=1}^{\infty}\frac{c_n}{k_n}\left(\sinh(k_n x) - \tanh(\tfrac{1}{2}k_n L)\,\cosh(k_n x)\right)\psi_n(y)\,. \tag{5.24}$$

At the $1:1$ resonance, the two parameters $A_0^{(1)}$ and $\widehat{\theta}$ are arbitrary. The solutions with $\widehat{\theta} = 0$ are the free oscillations with the vessel stationary and no contribution from the evanescent modes. The solutions with $A_0^{(1)} = 0$ are quite different in that the fluid motion and vessel motion are coupled. There is then a continuum of mixed modes obtained by taking arbitrary values of $A_0^{(1)}$ and $\widehat{\theta}$ (determined by the choice of initial data).

6 Proof of equivalence of the two representations

The strategy for showing equivalence between the cosine expansion (4.6) and the vertical eigenfunction expansion (5.1) is to expand the $y-$dependence of (4.6) in terms of the vertical eigenfunctions and expand the $x-$dependent functions $A_n(x)$ in (5.1) in terms of a cosine series, and then compare the two. This strategy for the proof was suggested to the authors by McIver [22].

For simplicity restrict to non-resonant modes. The extension to resonant modes follows the same lines.

The cosine expansion with $b_n = 0$ can be written in the form

$$\widehat{\phi}(x,y) = \ell\omega\widehat{\theta}\sum_{m=0}^{\infty} p_m\, f_m(y)\, \cos(\alpha_m x)\,, \tag{6.1}$$

with

$$f_m(y) = 1 + \left(\frac{K}{K_m - K}\right)\frac{\cosh(\alpha_m y)}{\cosh(\alpha_m h_0)}\,, \tag{6.2}$$

where

$$K := \frac{\omega^2}{g} \quad \text{and} \quad K_m := \alpha_m \tanh(\alpha_m h_0)\,,$$

and $p_m = -4/L\alpha_n^2$ are the coefficients of the cosine expansion of $x - L/2$ in (4.5). Expand $f_m(y)$ in terms of the vertical eigenfunctions

$$f_m(y) = 1 + \left(\frac{K}{K_m - K}\right)\frac{\cosh(\alpha_m y)}{\cosh(\alpha_m h_0)} = \sum_{n=0}^{\infty} F_n^{(m)}\,\psi_n(y)\,. \tag{6.3}$$

The coefficients $F_n^{(m)}$ are determined using the formulae (B-9)

$$F_0^{(m)} = c_0\,\frac{\alpha_m^2}{\alpha_m^2 - k_0^2} \quad \text{and} \quad F_n^{(m)} = c_n\frac{\alpha_m^2}{k_n^2 + \alpha_m^2}\,. \tag{6.4}$$

Similarly expand the functions $A_0(x)$ in (5.8) (using (5.6)) and $A_n(x)$ in (5.9). For $A_0(x)$,

$$A_0(x) := \ell\omega\widehat{\theta}\frac{c_0}{k_0}\big(\sin(k_0 x) - \tan\left(\tfrac{1}{2}k_0 L\right)\cos(k_0 x)\big) = \sum_{m=0}^{\infty} u_m\,\cos(\alpha_m x)\,, \tag{6.5}$$

with

$$u_m = \ell\omega\widehat{\theta}c_0 p_m\frac{\alpha_m^2}{\alpha_m^2 - k_0^2}\,. \tag{6.6}$$

Similarly, using (5.9),

$$A_n(x) = \ell\omega\widehat{\theta}\frac{c_n}{k_n}\big(\sinh(k_n x) - \tanh\left(\tfrac{1}{2}k_n L\right)\cosh(k_n x)\big) = \sum_{m=0}^{\infty} U_m^{(n)}\,\cos(\alpha_m x)\,, \tag{6.7}$$

with

$$U_m^{(n)} = \ell\omega\widehat{\theta}c_n p_m\frac{\alpha_m^2}{k_n^2 + \alpha_m^2}\,. \tag{6.8}$$

To show equivalence between the two representations start with the cosine expansion. Substitute the vertical eigenfunction expansion for $f_m(y)$, reverse the order of summation, and then substitute the cosine expansion of the sequence of functions $A_n(x)$. The result

is the vertical eigenfunction representation. Carrying out the above steps:

$$
\begin{aligned}
\widehat{\phi}(x,y) &= \ell\omega\widehat{\theta}\big(x-\tfrac{1}{2}L\big)+\sum_{n=0}^{\infty}a_n\frac{\cosh(\alpha_n y)}{\cosh(\alpha_n h_0)}\,\cos(\alpha_n x)\\
&= \ell\omega\widehat{\theta}\sum_{n=0}^{\infty}p_n\cos(\alpha_n x)+\ell\omega\widehat{\theta}\sum_{n=0}^{\infty}p_n\left(\frac{K}{K_n-K}\right)\frac{\cosh(\alpha_n y)}{\cosh(\alpha_n h_0)}\,\cos(\alpha_n x)\\
&= \ell\omega\widehat{\theta}\sum_{n=0}^{\infty}p_n f_n(y)\cos(\alpha_n x)\\
&= \ell\omega\widehat{\theta}\sum_{n=0}^{\infty}\sum_{m=0}^{\infty}p_n F_m^{(n)}\psi_m(y)\,\cos(\alpha_n x)\\
&= \ell\omega\widehat{\theta}\sum_{m=0}^{\infty}\sum_{n=0}^{\infty}p_m F_n^{(m)}\psi_n(y)\,\cos(\alpha_m x)\\
&= \ell\omega\widehat{\theta}\sum_{m=0}^{\infty}p_m F_0^{(m)}\psi_0(y)\,\cos(\alpha_m x)+\ell\omega\widehat{\theta}\sum_{n=1}^{\infty}\sum_{m=0}^{\infty}p_m F_n^{(m)}\psi_n(y)\,\cos(\alpha_m x)\\
&= \ell\omega\widehat{\theta}c_0\psi_0(y)\sum_{m=0}^{\infty}p_m\frac{\alpha_m^2}{\alpha_m^2-k_0^2}\cos(\alpha_m x)+\ell\omega\widehat{\theta}\sum_{n=1}^{\infty}\sum_{m=0}^{\infty}p_m c_n\frac{\alpha_m^2}{k_n^2+\alpha_m^2}\psi_n(y)\,\cos(\alpha_m x)\\
&= \psi_0(y)\sum_{m=0}^{\infty}u_m\cos(\alpha_m x)+\sum_{n=1}^{\infty}\sum_{m=0}^{\infty}U_m^{(n)}\psi_n(y)\,\cos(\alpha_m x)\\
&= \left[\sum_{m=0}^{\infty}u_m\cos(\alpha_m x)\right]\psi_0(y)+\sum_{n=1}^{\infty}\left[\sum_{m=0}^{\infty}U_m^{(n)}\cos(\alpha_m x)\right]\psi_n(y)\\
&= A_0(x)\psi_0(y)+\sum_{n=1}^{\infty}A_n(x)\psi_n(y)\,,
\end{aligned}
$$

which is the representation of $\widehat{\phi}$ in terms of vertical eigenfunction expansion. This completes the transformation from the cosine expansion to the vertical eigenfunction expansion.

A similar argument can show that characteristic functions $\mathrm{D}^{\cos}(s)$ and $-\mathrm{D}^{\mathrm{vert}}(s)$ are equivalent (the form of $\mathrm{D}^{\mathrm{vert}}(s)$ in (5.14) must be multiplied by -1 in order to show equivalence). The main aspect of the proof is to show that the horizontal momentum of the fluid $\mathsf{M}^{\mathrm{horz}}$ is equivalent for each expansion. The detailed proof of this is given in the technical report [7], and the main result quoted here is

$$
\mathsf{M}^{\mathrm{horz}}=m_f\left[1-\frac{1}{h_0L}\sum_{n=0}^{\infty}2\frac{p_n}{\alpha_n^2}\left(\frac{KK_n}{K_n-K}\right)\right]=m_f\left[2\frac{c_0^2}{k_0L}\tan\left(\tfrac{1}{2}k_0L\right)+\sum_{n=1}^{\infty}2\frac{c_n^2}{k_nL}\tanh\left(\tfrac{1}{2}k_nL\right)\right].
$$

The equivalence of the two characteristic functions (4.13) and (5.14) is now clear by

writing

$$\begin{aligned}
\mathrm{D}^{\cos} &= \Big((m_v+m_f)\frac{g}{\omega}-m_v\ell\omega\Big)-\ell\omega m_f-\frac{8\ell m_f\omega^3}{L^2h_0g}\sum_{n=0}^{\infty}\frac{1}{\alpha_n^2}\frac{\tanh\alpha_nh_0}{\alpha_n\tanh\alpha_nh_0-\omega^2/g}\,,\\
&= \Big((m_v+m_f)\frac{g}{\omega}-m_v\ell\omega\Big)-\ell\omega m_f\left[1-\frac{1}{h_0L}\sum_{n=0}^{\infty}2\frac{p_n}{\alpha_n^2}\left(\frac{KK_n}{K_n-K}\right)\right],\\
&= \Big((m_v+m_f)\frac{g}{\omega}-m_v\ell\omega\Big)-\ell\omega m_f\left[2\frac{c_0^2}{k_0L}\tan\left(\tfrac{1}{2}k_0L\right)+\sum_{n=1}^{\infty}2\frac{c_n^2}{k_nL}\tanh\left(\tfrac{1}{2}k_nL\right)\right],\\
&= \Big((m_v+m_f)\frac{g}{\omega}-m_v\ell\omega\Big)-\frac{2\ell\omega m_fc_0^2}{k_0L}\tan\left(\tfrac{1}{2}k_0L\right)-2\ell\omega m_f\sum_{n=1}^{\infty}\frac{c_n^2}{k_nL}\tanh\left(\tfrac{1}{2}k_nL\right)\Bigg],\\
&= -\mathrm{D}^{\mathrm{vert}}.
\end{aligned}$$

7 Numerical evaluation of the characteristic equation

The roots of $\mathrm{P}(s)=0$ in all cases can be determined analytically. Finding the roots of $\mathrm{D}(s)=0$ for the full cosine expansion or the vertical eigenfunction expansion requires numerical solution. The simplest way to get approximate values for the real roots $\mathrm{D}(s)$ is to plot them as functions of s. The approximate values can then be refined if necessary using Newton's method.

Either $\mathrm{D}^{\cos}$ and $\mathrm{D}^{\mathrm{vert}}$ can be used to study the roots since they are equivalent. Even though they are equivalent there are some contexts where one or the other is better suited for analysis. For example the vertical eigenfunction expansion converges faster than the cosine expansion. When looking at weakly nonlinear theory (see comments in Concluding Remarks section below) the vertical eigenfunction expansion may be simpler. Hence it is of value to have a numerical algorithm for finding the roots of both $\mathrm{D}^{\cos}=0$ and $\mathrm{D}^{\mathrm{vert}}=0$. Finding the roots of $\mathrm{D}^{\cos}=0$ is much easier than finding the roots of $\mathrm{D}^{\mathrm{vert}}=0$ and so we will present the results for that case.

The principal difficulty in the search for roots of $\mathrm{D}^{\mathrm{vert}}=0$ is computing the wavenumbers $k_0(s)$ and $k_n(s)$, for $n=1,2,\ldots$. The obvious numerical strategy is to solve the transcendental equation $\mathsf{C}(\lambda)=0$ in (B-1). Firstly, this approach requires an accurate initial guess for each wavenumber for the iterative method to converge, and secondly one must be certain that no wavenumbers are missed.

Other approximate and numerical methods for computing these wavenumbers have been developed. For example, Chamberlain & Porter [10] compute approximations for the wavenumbers by constructing an integral equation for the eigenfunctions and then solving the integral equation both analytically and numerically. We use a similar strategy, except we approximate the differential equation (5.2) directly. Since the domain is finite, Chebyshev polynomial expansions can be used to approximate the $\psi_n(y)$ eigenfunctions for each n with high accuracy.

7.1 Spectral solution of the vertical eigenfunctions

Fix G, R and δ. Then at each value of s, the values of $k_0(s)$ and $k_m(s)$ need to be determined for $m=1,..,M$, where M is a large enough integer such that $\mathrm{D}^{\mathrm{vert}}$ is

independent of M. The strategy here is to expand the eigenfunctions $\psi_n(y)$ in a series of Chebyshev polynomials (cf. BOYD [9]), converting (5.2) to a matrix eigenvalue problem. Then a global eigenvalue solver gives all the eigenvalues up to the degree of the Chebyshev polynomial. In this approach the $y-$domain is transformed from $y \in [0, h_0]$ to $\bar{y} \in [-1, 1]$ and we express ψ as

$$\psi(\bar{y}) = \sum_{i=0}^{N_C} \gamma_i T_i(\bar{y}),$$

where $T_i(\bar{y})$ are Chebyshev polynomials, and γ_i are undetermined parameters. Evaluating this expression at the $N_C - 1$ collocation points

$$\bar{y}_i = \cos\left(\frac{i\pi}{N_C}\right), \quad i = 1, ..., N_C - 1,$$

and at the two boundaries $\bar{y} = -1$ and $\bar{y} = 1$, gives $N_C + 1$ algebraic equations for the eigenvalues λ, reducing (5.2) to the matrix eigenvalue problem

$$\mathbf{A}\Psi = \lambda\Psi\,, \quad \Psi \in \mathbb{R}^{N_c+1}\,.$$

The eigenvalues of $\mathbf{A}$ are then found via a standard QR-algorithm. We used the standard QR eigenvalue solver from LAPACK. The main benefit of this approach is that all the required eigenvalues, and hence the values of $k_0, k_1, \ldots$ are calculated in one go, without missing any. By choosing N_c large enough, the first M modes can be calculated to the desired accuracy.

The results in this paper use $M = 10$ evanescent modes, and so using $N_C = 50$ in the spectral collocation approach above is sufficient to calculate the values of $k_0, k_1, \ldots$ to 12 significant figures. These computed values were checked against values calculated via an iterative solution of (B-1).

7.2 Plotting $\mathrm{D}^{\mathrm{vert}}(s)$ as a function of s

Fix the resonance number at $m = 1$. $\mathrm{D}^{\mathrm{vert}}$ is plotted in Figure 5 as a function of s. Once a root of $\mathrm{D}^{\mathrm{vert}}(s) = 0$ is found, the values of $k_0, k_1, \ldots$ at that point can then be used to plot other features such as the surface elevation $h(x, t)$. The function $\mathrm{D}^{\mathrm{vert}}$ is infinite at the singularities which occur at the values

$$s^2 = \frac{(2n+1)\pi}{4\delta} \tanh((2n+1)\pi\delta)\,. \tag{7.1}$$

We have also plotted $\mathrm{D}^{\cos}(s)$ as a function of s and the graphs are identical to the graphs in Figure 5.

In the shallow water limit, Figure 5(a), the roots of the dispersion relation are evenly spaced, as there is negligible contribution from the evanescent modes in this limit. While for a finite depth fluid in Figure 5(b), the spacing between the roots of the characteristic function reduces as s increases due to the presence of evanescent modes.

7.3 Effect of coupling on free surface mode shapes

The free surface mode shapes for the first anti-symmetric and first symmetric free oscillation modes are just simple cosine functions (cf. Figure 3).

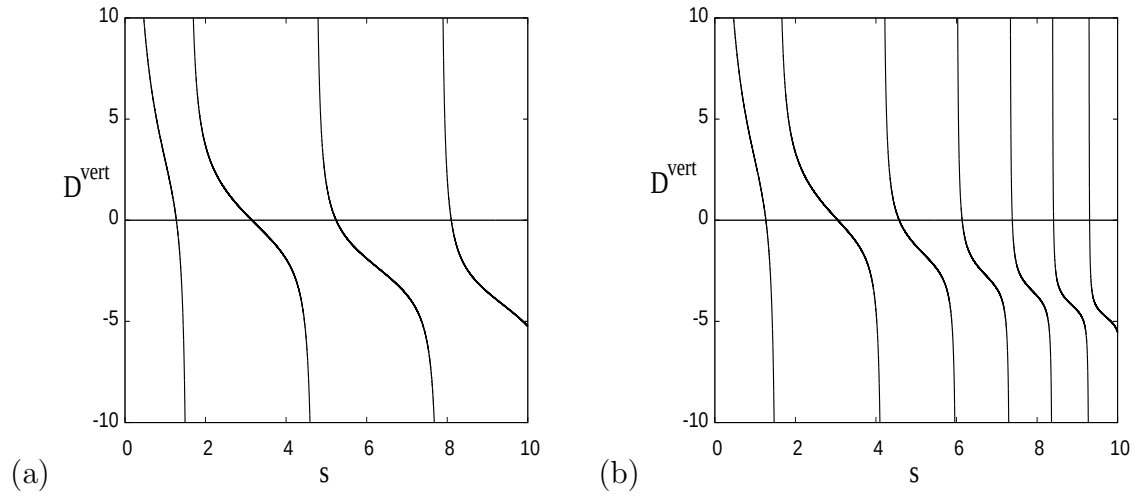

Figure 5: Characteristic function $\mathrm{D}^{\mathrm{vert}}(s)$ plotted as a function of s with $G = 5$ and $R = \frac{1}{2}$ for (a) $\delta = 0.01$ and (b) $\delta = 0.1$.

When the fluid motion is coupled to the vessel motion the free surface can be much more complicated since the full Fourier series or full eigenfunction expansion comes into play. In this section some mode shapes for the free surface when it is fully coupled are presented. The free surface mode shapes are defined in (2.14). Using the representation in terms of the vertical eigenfunctions the non-dimensional free surface mode shape is

$$\frac{h(x/L)}{h_0} = 1 + \frac{(1+R)s^2}{G\delta} \sum_{n=0}^{\infty} \widehat{A}_n(x/L)\psi_n(h_0)\,.$$

In the fully coupled non-resonant case,

$$\begin{aligned} \widehat{A}_0(x/L) &= \widehat{\theta}\frac{c_0}{k_0 L}\left(\sin(Lk_0x/L) - \tan(\tfrac{1}{2}k_0L)\cos(Lk_0x/L)\right) \\ \widehat{A}_n(x/L) &= \widehat{\theta}\frac{c_n}{k_n L}\left(\sinh(Lk_nx/L) - \tanh(\tfrac{1}{2}k_nL)\cosh(Lk_nx/L)\right)\,, \quad n \geq 1\,. \end{aligned}$$

Examples are shown in Figure 6. Although a very large number of terms is included the effect of the higher modes on the free surface shape is minor. The free surface shape for the coupled modes is still very close to a cosine function.

7.4 Numerics of the resonant characteristic equation

Consider the full characteristic function Δ^{vert} with both products included. Then a $1:1$ resonance occurs when Δ^{vert} and its first derivative vanish

$$\Delta^{\mathrm{vert}}(s) = \frac{d}{ds}\Delta^{\mathrm{vert}}(s) = 0\,.$$

In Figure 7 the function Δ^{vert} is plotted as a function of s. The first zero is simple, and the second zero is double since the curve is tangent to the horizontal axis. This second root is an example of the $1:1$ resonance. The parameter values are given in the caption.

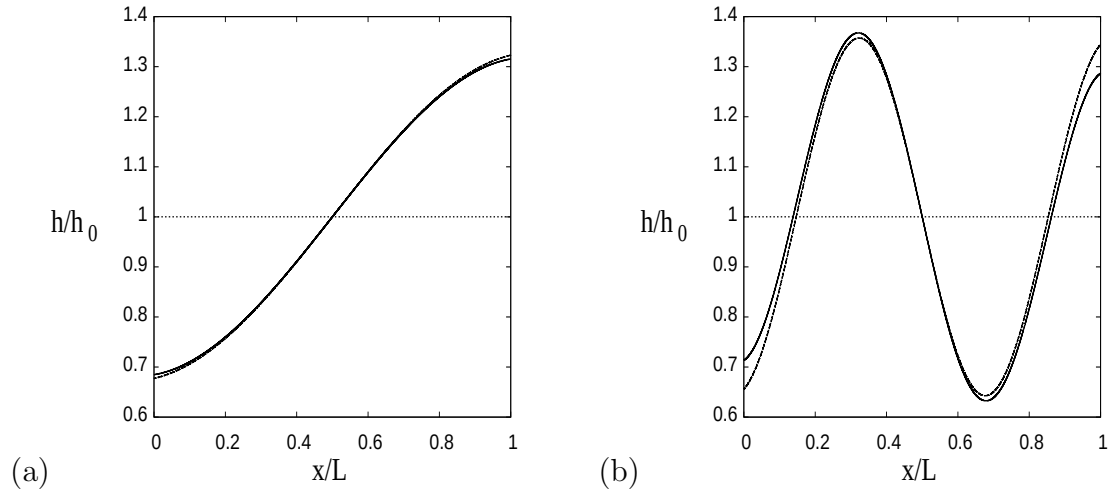

Figure 6: A plot of the free surface when $G = 5\,,\ R = 0.5\,,\ \delta = 0.5\,,$ and $\widehat{\theta} = \pi/20$ for (a) the 1st root of the characteristic function $\mathrm{D}^{\mathrm{vert}}(s)$ and (b) the second root of $\mathrm{D}^{\mathrm{vert}}(s)$. The solid line is the profile including evanescent modes and he dashed line is just the wave mode and the dotted line is $y = 1\,.$

8 Concluding remarks

To get some idea of the implications of the $1:1$ resonance for the nonlinear problem we can appeal to other problems with a $1:1$ resonance. The physical problem closest to the current model is the $1:1$ resonance in the Faraday experiment, when the vessel has a square or nearly-square horizontal cross-section. This configuration has been studied by Feng & Sethna [15]. The $1:1$ resonance is caused there by the square cross section, so physically it is very different from the mechanism for $1:1$ resonance here. However, mathematically it is very similar. To simplify notation, let

$$A := A_0^{(1)} \quad \text{and} \quad B := \widehat{\theta}\,.$$

Then the strategy for analyzing the weakly nonlinear problem is to introduce a slow time parameter

$$\tau = \varepsilon^2 t\,,$$

where ε is a measure of the amplitude of motion. Then let A and B depend on the slow time variable: $A(\tau)$ and $B(\tau)$. Then substitution into the nonlinear equations and carrying out an amplitude expansion leads to amplitude equations at third order of the form

$$\begin{aligned} \mathrm{i}A_\tau &= a_1 A + a_2|A|^2A + a_3|B|^2A + a_4B^2A \\ \mathrm{i}B_\tau &= b_1 B + b_2|B|^2B + a_3|A|^2B + a_4A^2B\,, \end{aligned} \tag{8.1}$$

with real parameters a_j, b_j. At resonance $a_1 = b_1$, and so $b_1 - a_1$ is a measure of the unfolding from resonance. According to results in [15] and [16] an analysis of solutions of this normal form shows that the weakly nonlinear solutions near resonance can be expected to include pure modes, mixed modes, secondary branches, connecting heteroclinic orbits, and heteroclinic cycles. Since A is associated with fluid motion and B is associated with vessel motion, a heteroclinic orbit is a mechanism for energy transfer between fluid and vessel.

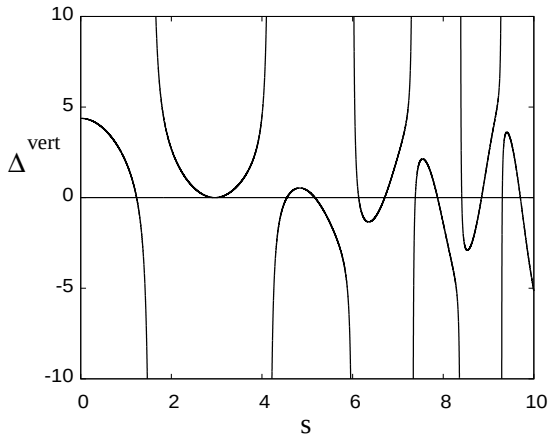

Figure 7: Plot of the characteristic function $\Delta^{\text{vert}}(s)$ for $G = 4.376$, $R = 0.5$ and $\delta = 0.1$. The double root of the dispersion relation at $s = s_m = 2.958$ denotes a $1:1$ resonance.

Another example, which has similarities to the Cooker experiment, and shows how weakly nonlinear analysis near a resonance causes energy transfer between modes, is the problem of a suspended elastic beam (Struble & Heinbockel [25]). In this model an elastic beam is suspended by two rigid cables free to rotate in the plane. The elastic beam is the analogue of the fluid in Cooker's experiment. The governing equations are quite different (for example the linearized equations completely decouple in [25]). However, there is a resonance, and their weakly nonlinear analysis shows that there are heteroclinic connections between solutions which are pathways to energy transfer.

Transfer of energy from non-symmetric to symmetric modes can also arise without resonance when forcing and nonlinearity are added. An example in the context of sloshing is the analysis of Feng [14], where a modal expansion with one symmetric and one nonsymmetric mode under the influence of forcing is studied. This mechanism, and its analysis, is however very different from the internal resonance mechanism without forcing.

Electronic version of the technical reports [6, 7, 8] can be downloaded at the website [1].

Acknowledgements

The authors are grateful to Professor Phil McIver of Loughborough University for suggesting the proof of equivalence [22] used in §6.

— Appendix —

A Derivation of the vessel equation

In this appendix the form of the vessel equation (1.1) is confirmed. First note that the Euler equations for the fluid relative to the moving frame are [8]

$$\frac{Du}{Dt} + \frac{1}{\rho}\frac{\partial p}{\partial x} = -\ddot{q}_1 \quad \text{and} \quad \frac{Dv}{Dt} + \frac{1}{\rho}\frac{\partial p}{\partial y} = -g - \ddot{q}_1\,, \tag{A-1}$$

where $q_1(t) = \ell\sin(\theta(t))$ and $q_2(t) = -\ell\cos(\theta(t))$. Substitute the Euler equations into (1.1), and use Reynold's transport theorem, to eliminate the pressure giving

$$\ddot{\theta} + \frac{g}{\ell}\sin\theta = -\frac{1}{(m_v+m_f)\ell}\left(\dot{\mathscr{C}}_1\cos\theta + \dot{\mathscr{C}}_2\sin\theta\right)\,, \tag{A-2}$$

where

$$\mathscr{C}_1 = \int_0^L\int_0^h \rho u\,\mathrm{d}y\mathrm{d}x \quad \text{and} \quad \mathscr{C}_2 = \int_0^L\int_0^h \rho v\,\mathrm{d}y\mathrm{d}x\,. \tag{A-3}$$

The equation (1.1) can be confirmed by using Newton's law with constraints. Here we will derive the equivalent version (A-2) using a variational principle (cf. Chapter 7 of Alemi Ardakani [2]).

The kinetic energy of the system is

$$KE = \frac{1}{2}\int_0^L\int_0^h \rho[(u+\dot{q}_1)^2 + (v+\dot{q}_2)^2]\,\mathrm{d}y\mathrm{d}x + \frac{1}{2}m_v(\dot{q}_1^2+\dot{q}_2^2)\,,$$

and the potential energy is

$$PE = \int_0^L\int_0^h \rho g(y-d+q_2)\,\mathrm{d}y\mathrm{d}x + \int\int_{\text{vessel}} \rho^{\text{vessel}} g(y-d+q_2)\,\mathrm{d}x\mathrm{d}y\,.$$

Let $\mathscr{L} = KE - PE$ and express q_1 and q_2 in terms of θ, and use the identities

$$m_f = \int_0^L\int_0^h \rho\,\mathrm{d}y\mathrm{d}x \quad \text{and} \quad m_v = \int\int_{\text{vessel}} \rho^{\text{vessel}}\,\mathrm{d}x\mathrm{d}y\,.$$

The Euler-Lagrange equation for θ is then

$$\begin{aligned}\frac{d}{dt}\left(\frac{\partial\mathscr{L}}{\partial\dot{\theta}}\right) - \frac{\partial\mathscr{L}}{\partial\theta} &= \frac{d}{dt}\left((m_v+m_f)\ell^2\dot{\theta} + \ell\mathscr{C}_1\cos\theta + \ell\mathscr{C}_2\sin\theta\right)\\ &\qquad - \left(-\mathscr{C}_1\ell\sin\theta\dot{\theta} + \mathscr{C}_2\ell\cos\theta\dot{\theta} - (m_v+m_f)g\ell\sin\theta\right)\\ &= (m_v+m_f)\ell^2\ddot{\theta} + \dot{\mathscr{C}}_1\ell\cos\theta + \dot{\mathscr{C}}_2\ell\sin\theta + (m_v+m_f)g\ell\sin\theta\,.\end{aligned}$$

Dividing by $(m_v+m_f)\ell^2$ then confirms the form of the vessel equation (A-2).

This Lagrangian is quite satisfactory for deriving the equations for the vessel motion, but it does not give the correct equation for the fluid motion. The Lagrangian can be modified by adding constraints to give the fluid equations (see [2]), but a variational principal for the fluid motion will not be needed in this paper.

B The vertical eigenfunctions

The eigenvalue problem for the vertical eigenfunctions is recorded in (5.2) with λ the eigenvalue parameter, and ω^2/g is treated as a given real parameter. Here the properties of the eigenvalues and eigenfunctions are recorded following [21].

This eigenvalue problem can be solved analytically, but the characteristic equation, $\mathsf{C}(\lambda) = 0$, for the eigenvalue λ is transcendental, where

$$\mathsf{C}(\lambda) = \frac{\omega^2 h_0}{g} \cos\left(h_0\sqrt{\lambda}\right) + \left(h_0\sqrt{\lambda}\right) \sin\left(h_0\sqrt{\lambda}\right). \tag{B-1}$$

The function $\mathsf{C}(\lambda)$ is real for all λ, $\mathsf{C}(0) > 0$ and $\mathsf{C}(\lambda) \to -\infty$ as $\lambda \to -\infty$. There is exactly one negative eigenvalue

$$\lambda_0 = -k_0^2, \tag{B-2}$$

where k_0 is the unique root of

$$k_0 h_0 \tanh(k_0 h_0) - \frac{\omega^2 h_0}{g} = 0, \tag{B-3}$$

for any fixed $\omega^2 h_0/g$. The mode k_0 is associated with the *wave mode*.

In addition there is a countable number of positive eigenvalues

$$\lambda_n = k_n^2, \quad n = 1, 2, \dots, \tag{B-4}$$

(see Figure 2.1 in [21]) with the sequence k_n determined by

$$k_n h_0 \tan(k_n h_0) + \frac{\omega^2 h_0}{g} = 0, \quad n = 1, 2, \dots. \tag{B-5}$$

The modes k_n for $n \geq 1$ are associated with *evanescent modes*.

The associated eigenfunctions are

$$\psi_0(y) = \frac{1}{N_0} \cosh(k_0 y) \quad \text{and} \quad \psi_n(y) = \frac{1}{N_n} \cos(k_n y), \quad n = 1, 2, \dots, \tag{B-6}$$

with

$$N_0 = \sqrt{\frac{1}{2}\left(1 + \frac{\sinh 2k_0 h_0}{2k_0 h_0}\right)} \quad \text{and} \quad N_n = \sqrt{\frac{1}{2}\left(1 + \frac{\sin 2k_n h_0}{2k_n h_0}\right)}. \tag{B-7}$$

The coefficients N_0 and N_n are chosen so that the eigenfunctions have unit norm,

$$\frac{1}{h_0}\int_0^{h_0} \psi_n(y)^2 \, \mathrm{d}y = 1, \quad n = 0, 1, 2, \dots. \tag{B-8}$$

The set $\{\psi_0(y), \psi_1(y), \dots\}$ is complete on the interval $[0, h_0]$. Hence any square-integrable function $g(y)$ on this interval can be expanded in a series

$$g(y) = \sum_{n=0}^{\infty} g_n \psi_n(y), \quad \text{with} \quad g_n = \frac{1}{h_0}\int_0^{h_0} g(y)\, \psi_n(y) \, \mathrm{d}y. \tag{B-9}$$

References

[1] http://personal.maths.surrey.ac.uk/st/T.Bridges/SLOSH/RESONANCE/

[2] H. Alemi Ardakani. *Rigid-body motion with interior shallow-water sloshing*, PhD Thesis, Department of Mathematics, University of Surrey (2010).

[3] H. Alemi Ardakani & T.J. Bridges. *Dynamic coupling between shallow-water sloshing and horizontal vehicle motion*, Euro. J. Appl. Math. **21** 479–517 (2010).

[4] H. Alemi Ardakani & T.J. Bridges. *Shallow-water sloshing in vessels undergoing prescribed rigid-body motion in three dimensions*, J. Fluid Mech. **667** 474–519 (2011).

[5] H. Alemi Ardakani & T.J. Bridges. *Shallow-water sloshing in vessels undergoing prescribed rigid-body motion in two dimensions*, Euro. J. Mech. B/Fluids **31** 30–43 (2012).

[6] H. Alemi Ardakani & T.J. Bridges. *1:1 resonance in the shallow-water model for Cooker's sloshing experiment*, Technical Report, University of Surrey (2012). Electronic copy available at [1].

[7] H. Alemi Ardakani, T.J. Bridges & M.R. Turner. *Details of the proof of equivalence: the "cosine" versus "vertical eigenfunction" representations*, Technical Report, University of Surrey (2012). Electronic copy available at [1].

[8] H. Alemi Ardakani, T.J. Bridges & M.R. Turner. *Resonance in a model for Cooker's sloshing experiment – the extended version*, Technical Report, University of Surrey (2012). Electronic copy available at [1].

[9] J.P. Boyd. *Chebyshev and Fourier Spectral Methods*, Second Edition, Dover Publications: New York (2001).

[10] P.G. Chamberlain & D. Porter. *On the solution of the dispersion relation for water waves*, Appl. Ocean. Res. **21** 161–166 (1999).

[11] M.J. Cooker. *Water waves in a suspended container*, Wave Motion **20** 385–395 (1994).

[12] O.M. Faltinsen & A.N. Timokha. *Sloshing*, Cambridge University Press (2009).

[13] J.B. Frandsen. *Numerical predictions of tuned liquid tank structural systems*, J. Fluids & Structures **20** 309–329 (2005).

[14] Z.C. Feng. *Coupling between neighboring two-dimensional modes of water waves*, Phys. Fluids **10** 2405–2411 (1998).

[15] Z.C. Feng & P.R. Sethna. *Symmetry breaking bifurcations in resonant surface waves*, J. Fluid Mech. **199** 495–518 (1989).

[16] Z.C. Feng & P.R. Sethna. *Global bifurcation and chaos in parametrically forced systems with* 1 : 1 *resonance*, Dynamical Systems: an Inter. Journal **5** 201–225 (1990).

[17] E.W. Graham & A.M. Rodriguez. *The characteristics of fuel motion which affect airplane dynamics*, J. Appl. Mech. **19** 381–388 (1952).

[18] A. Herczyński & P.D. Weidman. *Experiments on the periodic oscillation of free oscillations driven by liquid sloshing*, J. Fluid Mech. **693** 216–242 (2012).

[19] R.A. Ibrahim. *Liquid Sloshing Dynamics*, Cambridge University Press (2005).

[20] T. Ikeda & N. Nakagawa. *Non-linear vibrations of a structure caused by water sloshing in a rectangular tank*, J. Sound Vibr. **201** 23–41 (1997).

[21] C.M. Linton & P. McIver. *Handbook of Mathematical Techniques for Wave-Structure Interaction*, Chapman & Hall/CRC: Boca Raton (2001).

[22] P. McIver. Private Communication (2012).

[23] H. Ockendon, J.R. Ockendon & D.D. Waterhouse. *Multi-mode resonances in fluids*, J. Fluid Mech. **315** 317–344 (1996).

[24] H. Ockendon & J.R. Ockendon. *Nonlinearity in fluid resonances*, Meccanica **36** 297–321 (2001).

[25] R.A. Struble & J.H. Heinbockel. *Resonant oscillations of a beam-pendulum system*, J. Appl. Mech. **30** 181–188 (1963).

[26] G.I. Taylor. *The interaction between experiment and theory in fluid mechanics*, Ann. Rev. Fluid Mech. **6** 1–17 (1974).

[27] J.-M. Vanden-Broeck. *Nonlinear gravity-capillary standing waves in water of arbitrary uniform depth*, J. Fluid Mech. **139** 97–104 (1984).

[28] J. Yu. *Effects of finite water depth on natural frequencies of suspended water tanks*, Stud. Appl. Math. **125** 373–391 (2010).